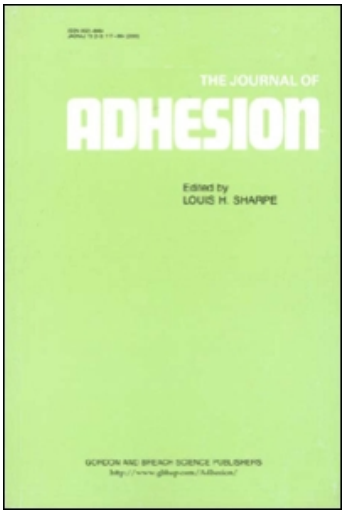


## The Journal of Adhesion

Publication details, including instructions for authors and subscription information:
http://www.informaworld.com/smpp/title~content=t713453635

# Elastoplastic Finite Element Analysis and Strength Evaluation of Adhesive Butt Joints of Similar and Dissimilar Hollow Shafts Subjected to External Bending Moments

Toshiyuki Sawa[a]; Mitsuhiro Aoki[a]; Osamu Nishikawa[a]
[a] Department of Mechanical Engineering, Yamanashi University, Yamanashi, Japan

**To cite this Article** Sawa, Toshiyuki , Aoki, Mitsuhiro and Nishikawa, Osamu(1997) 'Elastoplastic Finite Element Analysis and Strength Evaluation of Adhesive Butt Joints of Similar and Dissimilar Hollow Shafts Subjected to External Bending Moments', The Journal of Adhesion, 61: 1, 55 — 69
**To link to this Article: DOI:** 10.1080/00218469708010516
**URL:** http://dx.doi.org/10.1080/00218469708010516

*J. Adhesion*, 1997, Vol. 61, pp. 55–69
Reprints available directly from the publisher
Photocopying permitted by license only



# Elastoplastic Finite Element Analysis and Strength Evaluation of Adhesive Butt Joints of Similar and Dissimilar Hollow Shafts Subjected to External Bending Moments

TOSHIYUKI SAWA, MITSUHIRO AOKI and OSAMU NISHIKAWA

*Department of Mechanical Engineering, Yamanashi University, 4-3-11, Takeda, Kofu, Yamanashi 400, Japan*

*(Received 30 January 1996; In final form 24 April 1996)*



Stress distributions and deformation of adhesive butt joints are analyzed by an elastoplastic finite element method when the joints of similar and dissimilar shafts are subjected to external bending moments. The effects of the ratio of Young's modulus for the adherends to that for an adhesive and the effects of the adhesive thickness on the interface stress distribution are investigated. Joint strength is predicted by using the elastoplastic interface stress distributions. It is found that the singular stress at the edge of the interfaces increases with an increase of the ratio of Young's modulus. Measurement of strains in joints and experiments on joint strength were conducted. The numerical results are in fairly good agreement with the experimental results. It is observed that the joint strength for dissimilar shafts are smaller than those for similar shafts. A fracture of dissimilar adhesive up-bonded shafts occurred from the interface of the adherend with smaller Young's modulus. It is seen that joint strength increases as the adhesive thickness increases.

*Keywords:* Finite element analysis; elastoplasticity; adhesive butt joints; hollow shafts; dissimilar adherends; bending moments; interface stress distribution; strength evaluation

## 1. INTRODUCTION

Recently, adhesive joints have been used in mechanical structures as the performance of bonding materials has advanced. However, the design of the joints results almost entirely from experience. It is

desirable to establish an optimal design method for adhesive joints. In establishing the design method for adhesive joints, it is necessary to know the stress distributions in joints more precisely. Many investigations have been carried out on lap, scarf, and butt adhesive joints subjected to tensile, bending moment, cleavage, and torsional loads [1–5]. But these investigations have treated two-dimensional configuration joints and three-dimensional configuration joints subjected to axisymmetric loads [6–9], and few have been carried out on the mechanical behaviors of three-dimensional configuration joints consisting of similar and dissimilar adherends subjected to axiasymmetric loads such as bending moments. In practice, adhesive joints of hollow shafts have been used in the automobile and other industries where the joints are subjected to a bending moment as well as torsion. It is, therefore, necessary to know the stress distribution of adhesive joints consisting of similar and dissimilar hollow shafts subjected to bending moments.



In this paper, stress distributions of adhesive butt joints consisted of similar and dissimilar hollow shafts are analyzed by an elastoplastic finite element method when the joints are subjected to external bending moments. The effects of the ratio of Young's modulus of the adherends to that for an adhesive and the effects of the adhesive thickness on the interface stress distributions are investigated. Changes in yielded area at the interface are also shown with an increase of bending moment. Using the interface stress distributions, joint strength is estimated. For verification, measurement of strain in joints was conducted. Four-point bending tests were carried out to measure the joint strength. The analytical results are compared with the experimental ones.

## 2. METHOD OF ANALYSIS

Figure 1 shows an adhesive butt joint, consisted of two dissimilar finite hollow cylinders, subjected to an external bending moment. In order to know the stress distribution in adhesive [II], an elastoplastic finite element analysis is carried out. The adherends are denoted as finite hollow cylinders [I] and [III], and the adhesive as a finite hollow cylinder [II]. The inner diameter of cylinder [I] is designated

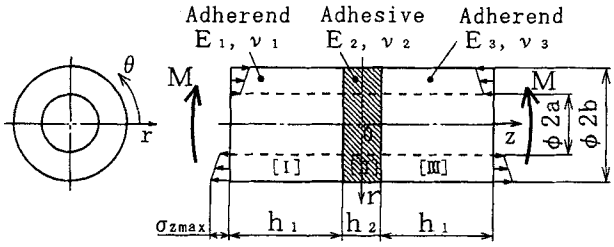


FIGURE 1 Adhesive butt joint of dissimilar hollow shaft subjected to external bending moment.

as $2a$ and the outer diameter as $2b$, the height as $h_1$, Young's modulus as $E_1$ and Poisson's ratio as $v_1$. Those for cylinder [II] are designated as $2a$, $2b$, $h_2$, $E_2$ and $v_2$, and those for cylinder [III] as $2a$, $2b$, $h_3$, $E_3$ and $v_3$, respectively. Figure 2 shows an example of the mesh (a half section of the adhesive joint) used in the FEM analysis. Hexahedron elements are employed. The number of finite elements and nodes employed are 2660 and 3432, respectively. When the inner diameter $2a$ is zero, that is, the case of a solid shaft, pentahedron and hexahedron elements are used. The numbers of elements and nodes are 2660 and 3042, respectively. The FEM code employed is KSWAD/FEM · SOLVE (KUBOTA, Co., Ltd.).

An external bending moment, M, is assumed to be applied with linear stress distribution $\sigma_z$ as shown Figure 1. It is assumed that the stress $\sigma_z$ acts linearly in the radial direction and sinusoidally in the circumferential direction on both ends of cylinders [I] and [III] within the region $a \leqslant r \leqslant b$ as shown in Figures 1 and 2. The absolute value

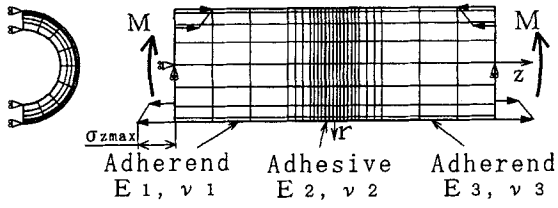


FIGURE 2 Boundary conditions and an example of the mesh used in FEM analysis.

at the position $r = b$ and $\theta = 3/2\pi$ is denoted as $\sigma_{z\max}$ as shown in Figures 1 and 2. A relationship between $\sigma_z$ and $M$ is expressed by Eq. (1)

$$M = 4\int_0^{\pi/2}\int_a^b \sigma_z r dr d\theta \tag{1}$$

where

$$\sigma_z = \sigma_{z\max}\cos\theta\frac{r}{b} \tag{2}$$

In the numerical calculations, the dimensions of the adhesive joints are chosen as $2a = 20$ [mm], $2b = 30$ [mm], $h_1 = 50$ [mm] $h_2 = 0.05$ [mm] and $h_3 = 50$ [mm]. The combinations of materials for adherends are steel and steel, aluminum and aluminum, and steel and aluminum, respectively. An epoxy adhesive which is solidified at room temperature was used. These combinations of adherend materials are denoted by St-St, Al-Al and St-Al. Table I shows the mechanical properties of adherends and adhesive. The stress-strain diagram is approximated as that of an elastic-linearly plastic body. The slope of the stress-strain diagram after yeilding denoted by $c$ and the value is shown in Table I. Figure 3 shows an example of the stress-strain diagram for the epoxy resin adhesive. The dotted line indicates an approximation as an elastic-linearly plastic body. The yield stress and the fracture stress of epoxy resin adhesive were obtained from experiments as 21.2 MPa and 28.1 MPa respectively.

TABLE I Mechanical properties of adherends and adhesive

| | *adherend (St)* | *adherend (Al)* | *adhesive (epoxy)* |
|---|---|---|---|
| Young's modulus E[GPa] | 205.8 | 71.5 | 3.63 |
| Poisson's ratio $\nu$ | 0.30 | 0.33 | 0.37 |
| Yield stress $\sigma$ Y[MPa] | 425.3 | 261.7 | 21.2 |
| c[GPa] | 19.8 | 9.00 | 0.0304 |

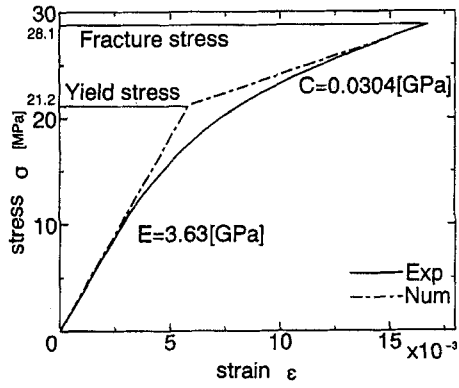


FIGURE 3 Stress-strain diagram (epoxy adhesive).



## 3. EXPERIMENTAL METHOD

Experiments were conducted to measure the strain at the outer surface of the adherend and the joint strength. Figure 4 shows the dimensions of the hollow shaft specimens. Solid shafts were also manufactured. The adherends were made of steel (S45C JIS) and aluminum (A5056 JIS). Figure 5 shows the positions of the strain gauges attached to the outer surface of the adherends. The solid and hollow shafts were bonded by an epoxide adhesive (SUMITOMO 3M, Co., Ltd., in Japan, Scotch Weld® 1838).

Figure 6 shows an experimental apparatus for four-point bending tests. When a force, $W$, is applied to the adhesive butt joints by a material testing machine, a bending moment, $M$ ( $= W/2 \times 50$), occurs.

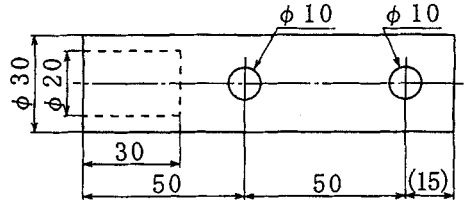


FIGURE 4 Geometry and dimensions (in mm) of solid and hollow shaft specimens used in experiments.

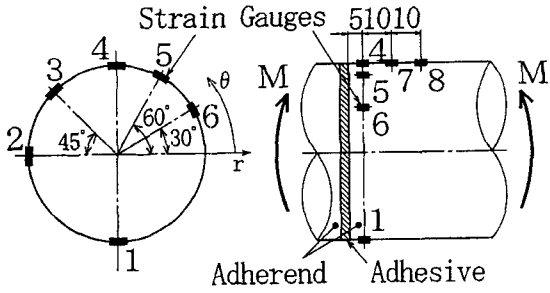


FIGURE 5 Attached positions of strain gauges.

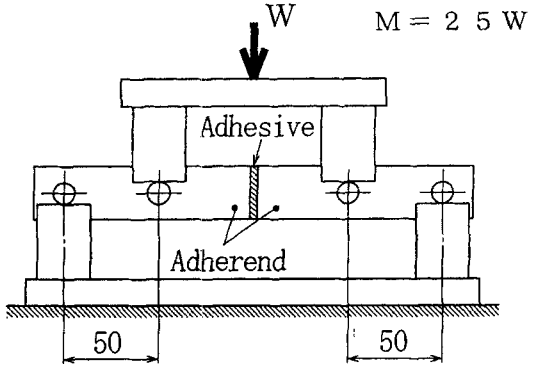


FIGURE 6 A schematic of the experimental apparatus.

The magnitude of the force, $W$, is measured with a load cell, and the strain in circumferential direction by the strain gauges attached to the shaft. The output signals are recorder by a $X-Y$ recorded through dynamic amplifiers.

## 4. RESULTS OF ANALYSIS AND COMPARISION WITH EXPERIMENT

### 4.1. Results of Analysis

Figure 7 shows the effect of the ratio of Young's modulus for the adherends to that for the adhesive, $E_1/E_2$, on the stress distributions

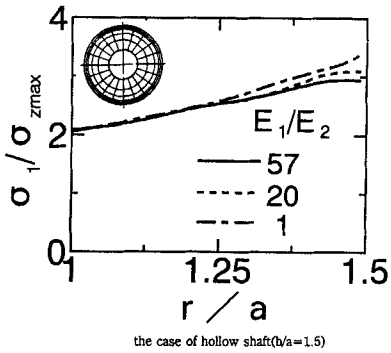


FIGURE 7 Effects of the ratio of Young's moduli, $E_1/E_2$, on the maximum principal stress distribution at the interface

$$\begin{pmatrix} h_2/b = 0.003,\ E_1/E_3 = 1,\ \theta = 3/2\pi \\ h_1 = h_3 = 50[\text{mm}],\ h_2 = 0.05[\text{mm}] \end{pmatrix}.$$

at the interface ($\theta = 3/2\pi$), where the values $E_1/E_2$ are chosen as 1, 20 and 57 and the adhesive butt joint consists of similar material ($E_1 = E_3$). The ordinate is the normalized maximum principal stress, $\sigma_1/\sigma_{z\max}$, where $\sigma_{z\max}$ is shown in the model of Figure 1 and the abscissa is the ratio of the distance from the center to the inner radius of the finite hollow cylinder. The stress distributions at the interface are shown at the angle $\theta = 3/2\pi$. This Figure shows the stress distribution at the interface where the stress of the element exceeds the yield stress and reaches the fracture stress of the adhesive near the point $r = b$ and $\theta = 3/2\pi$. Furthermore, the nodes of the elements for which the stress reaches the fracture stress are released in the analysis. At this moment, the magnitude of the external bending moment and yielded area are indicated in this Figure, where the solid black color indicates the yielded regions. It is seen that the maximum principal stress distribution of $\sigma_1$ near the outer diameter, $r/b = 1.5$, increases as the value $E_1/E_2$ approaches 1.

Figure 8 shows the stress distribution at the interface ($\theta = 3/2\pi$), when the ratio of Young's modulus of the adherends is held constant at $E_1/E_3 = 2.9$ (St-Al) and $E_1/E_2 = 57$. In addition, the stress distribution is indicated when the adherends are similar ($E_1/E_3 = 1$). The symbol I indicates the interface of the adherend with the larger Young's modulus and the symbol III indicates the opposite side inter-

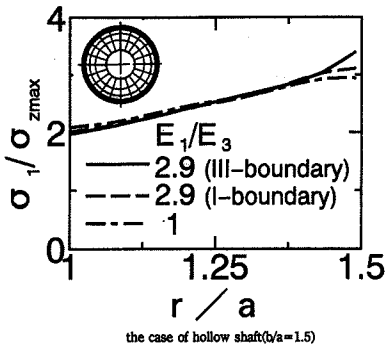


FIGURE 8 Effects of the ratio of Young's moduli, $E_1/E_3$, on the maximum principal stress distribution at the interface

$$\begin{pmatrix} h_2/b = 0.003,\ E_1/E_2 = 57,\ \theta = 3/2\pi \\ h_1 = h_3 = 50[\text{mm}],\ h_2 = 0.05[\text{mm}] \end{pmatrix}.$$

face. It is found that the normalized maximum principal stress becomes larger at the interface of the adherend with the smaller Young's modulus. It is also seen that the normalized maximum principal stress at the position of $r/a = 1.5$ and $\theta = 3/2\pi$ increases with an increase of the value $E_1/E_3$. In the case of dissimilar shafts, it is predicted that the joint fracture occurs at the interface of the adherend with the smaller Young's modulus because the principal stress is larger than that at the interface of the adherend with the larger Young's modulus. This result is different from the strength of a joint subjected to a tensile load [10]. In addition, it is predicted that the joint strength of dissimilar hollow shafts is smaller than that of similar hollow shafts.

Figure 9 shows the effect of the adhesive thickness on the stress distribution at the interface. The normalized maximum principal stress distribution near the edge of the outer diameter ($r/a = 1.5$) increases with a decrease of $h_2/b$. The results are the reverse of the characteristics of joints subjected to external tensile loads. In order to investigate the effects of tensile loads on the interface stress distributions, FEM analysis was performed. Figure 10 shows an example of mesh in the FEM analysis of the adhesive joint subjected to tensile loads. The joint geometry is similar to that subjected to bending moments. Figure 11 shows the effect of the ratio of Young's modulus for the adherends to that for the adhesive, $E_1/E_2$, on the maximum

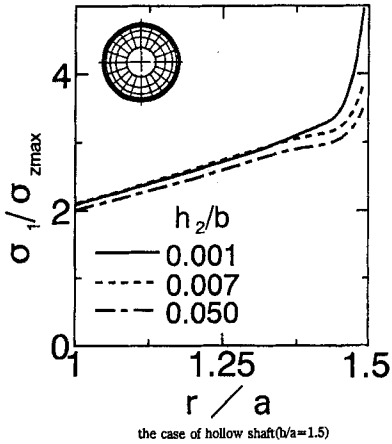


FIGURE 9 Effects of the adhesive thickness on the maximum principal stress distribution at the interface

$$\begin{pmatrix} E_1/E_2 = 57,\ E_1/E_3 = 1,\ \theta = 3/2\pi \\ h_1 = h_3 = 50[\text{mm}] \end{pmatrix}.$$

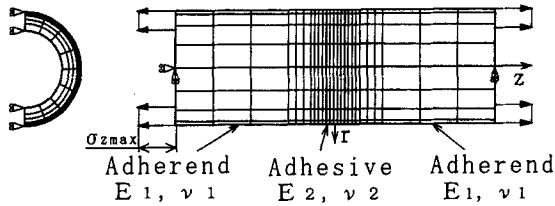


FIGURE 10 Boundary conditions and an example of the mesh used in FEM analysis when a tensile load is applied to an adhesive butt joint.

principal stress at the interface ($\theta = 3/2\pi$). Figure 12 shows the effect of the adhesive thickness on the maximum principal stress at the interface. In the case where the joints are subjected to tensile loads, a uniform stress distribution of $\sigma_{z\max}$, which is the maximum value in the case of bending moments, acts on the ends of the joints. From the comparisons between the cases of tensile loads and bending moments, it is seen that the results in the case where external bending moments are applied are opposite to those in the case where tensile loads are

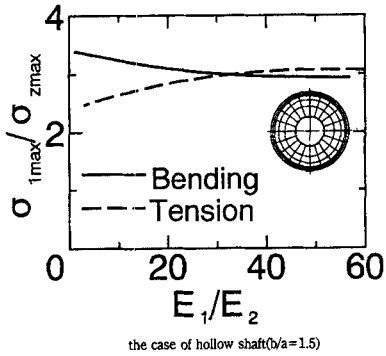


FIGURE 11 Effects of the ratio of Young's moduli, $E_1/E_2$, on the maximum principal stresses in both cases where bending moments and tensile loads are applied

$$\begin{pmatrix} h_2/b = 0.003,\ E_1/E_3 = 1,\ \theta = 3/2\pi \\ h_1 = h_3 = 50[\text{mm}],\ h_2 = 0.05[\text{mm}] \end{pmatrix}.$$

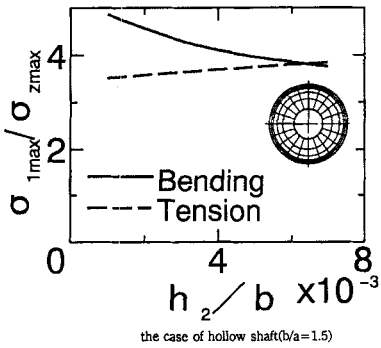


FIGURE 12 Effects of the adhesive thickness on the maximum principal stresses in both cases where bending moments and tensile loads are applied

$$\begin{pmatrix} E_1/E_2 = 57,\ E_1/E_3 = 1,\ \theta = 3/2\pi \\ h_1 = h_3 = 50[\text{mm}] \end{pmatrix}.$$

applied. It is found that the maximum principal stress, $\sigma_{1\max}$, increases when the value $E_1/E_2$ approaches 1 and the value $h_2/b$ decreases when joints are subjected to bending moments.

Figure 13 shows the changes in the normalized maximum principal stress at the interface of adherend III with smaller Young's modulus

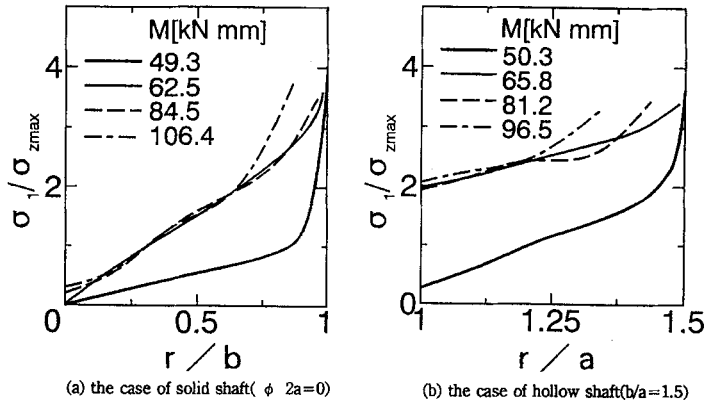


FIGURE 13 Changes in stress distribution at the interface with an increase of bending moment

$$\begin{pmatrix} h_2/b = 0.003,\ E_1/E_2 = 57,\ E_1/E_3 = 2.9,\ \theta = 3/2\pi \\ h_1 = h_3 = 50[\text{mm}],\ h_2 = 0.05[\text{mm}] \end{pmatrix}.$$

($\theta = 3/2\pi$) when bending moments are increased. When the maximum principal stress reaches the fracture stress of the adhesive, the nodes were released in this analysis. The interface stress distributions within the elastic regions are also indicated, that is, $M = 49.3\,\text{KN}\cdot\text{mm}$ in the case of Figure 13 (a) and $M = 50.3\,\text{KN}\cdot\text{mm}$ in the case of Figure 13 (b). From a comparison of the interface stress distribution between solid shaft and hollow shaft for the same outer diameter, the difference in the maximum principal stress is small but the difference in the slope of stress distributions is very different. Figure 14 shows changes in the yielded region at the interface of the adherend with the smaller Young's modulus with an increase of bending moment. In this paper, joint fracture is defined as being when the stress at the half part of the interface reaches the fracture stress. The difference in bending moment between when yield of the adhesives starts and when joint fracture occurs was very small. Thus, almost all nodes in the yielded area were released. The region of the yielded part progresses toward the center from the edge of the interface with an increase of the bending moment.

In the analysis, the stress-strain relationship is approximated as a linear-plastic body as shown in Figure 3. In order to obtain more realistic behavior of the joints, it is necessary to approximate the stress-strain relationship more precisely.

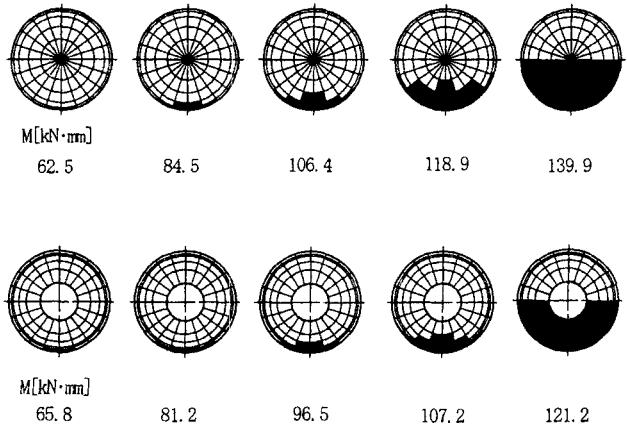


FIGURE 14 Changes in yield region at the interface with an increase of bending moment

$$\begin{pmatrix} h_2/b = 0.003,\ E_1/E_2 = 57,\ E_1/E_3 = 2.9 \\ h_1 = h_3 = 50[\text{mm}],\ h_2 = 0.05[\text{mm}] \end{pmatrix}.$$

## 4.2. Comparisons between Analytical and Experimental Results Concerning Strain

Figure 15 shows the comparison between the measured and the numerical results concerning strain in the adherends. The ordinate represents the strain, $\varepsilon z$, and the abscissa is the position, $\theta$, of the attached strain gauge. Taking into consideration the joint symmetry, the range of angle is taken as $0 \leqslant \theta \leqslant 90$. From Figure 15, a fairly good agreement between the numerical and the experimental result is found.

## 4.3. Comparisons between Analytical and Experimental Results on Joint Strength

The bending moment when joint fracture occurs is predicted by the procedure mentioned above, namely, the joint fracture is defined such that a half part of the interface reaches the fracture stress of the adhesive. Table II shows bending moments obtained by elastoplastic analysis (E-P), elastic analysis (E) and experimental results when fracture occurs. The experimental results indicate the average values of 20

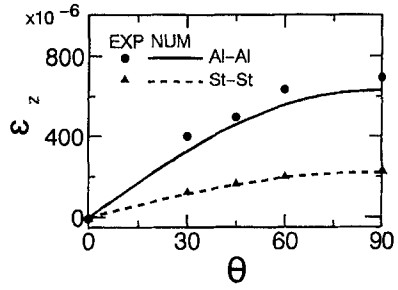


FIGURE 15 Comparisons between the numerical and the experimental results concerning strain of adherend ($M = 98\,\mathrm{KN}\cdot\mathrm{mm}$)

$$\begin{pmatrix} \phi \quad 2a = 20[\mathrm{mm}],\ \phi \quad 2b = 30[\mathrm{mm}] \\ h_1 = h_3 = 50[\mathrm{mm}],\ h_2 = 0.05[\mathrm{mm}] \end{pmatrix}.$$

TABLE II Comparisons between the numerical and the experimental results concerning joint strength (bending moment: $M$)
(a) Case of hollow shaft [KN·mm]

| | *St-St* | *Al-Al* | *St-Al* |
|---|---|---|---|
| Exp | 156 | 143 | 125 |
| Num (E-P) | 154.2 | 139.9 | 121.2 |
| Num (E) | 139.1 | 110.9 | 106.0 |

(a) Case of solid shaft [KN·mm]

| | *St-St* | *Al-Al* | *St-Al* |
|---|---|---|---|
| Exp | 175 | 162 | 143 |
| Num (E-P) | 174.3 | 158.9 | 139.9 |
| Num (E) | 171.6 | 140.2 | 130.8 |

four-point bending tests. The standard deviation of the experimental results is between 1.40 and 1.96 KN·mm. In the elastic finite element analysis, the joint fracture is defined such that the maximum principal stress at the edge of interface reaches the fracture stress obtained from cylinder specimen tests [11] and the bending moment is defined as the fracture strength of the joint. The fracture stress of cylinder specimens for St-St, Al-Al and St-Al were measured as 47.4MPa, 43.9MPa and 41.2MPa, respectively [11]. The adhesive joint strength of St-St is greater than that of the Al-Al adhesive joint in similar shafts. This

result agrees with the predicted values shown in Figure 7. It is found that the strength of similar shafts is greater than that of dissimilar shafts. This result agrees with the predicted values in Figure 8. From comparisons between the case of hollow shafts and the case of the solid shaft, for which the outer diameter is the same as for the hollow shafts, it is found that the joint strength of solid shafts is greater than that of hollow shafts. The predicted value of the bending moment for joint fracture obtained by elastoplastic finite element analysis (E-P) is in fairly good agreement with the experimental one.

With respect to elastic finite element analysis (E), the value of the bending moment is smaller than that from elastoplastic analysis. It was found experimentally that the joint fracture occurred (visually) at the interface. In the case of dissimilar shafts, the joint fracture occurred (visually) at the interface of the aluminum adherend. These results agree with those from elastoplastic analysis.



## 5. CONCLUSIONS

This paper dealt with the interfacial stress distributions and the strength evaluation of adhesively bonded butt joints of similar and dissimilar hollow shafts subjected to external bending moments. The following results were obtained.

(1) The interfacial stress distributions of adhesive butt joints consisting of dissimilar hollow shafts subjected to external bending moments were analyzed by an elastoplastic finite element method, and increases of the yielded area at the interface with increases in bending moment were indicated. It was, found that the maximum principal stress at the interface of the adherend with smaller Young's modulus is larger than that at the interface of the adherend with larger Young's modulus. In addition, it was seen that the maximum principal stress increases with a decrease of the ratio of Young's modulus for the adherend to that for the adhesive, $E_1/E_2$, and with a decrease of the adhesive thickness.

(2) Adhesive butt joints of similar and dissimilar hollow shafts subjected to tensile loads were also analyzed. It was found that the

characteristics of joints subjected to tensile loads are opposite of those of joints subjected to bending moments.

(3) Using the interfacial stress distributions, joint strength was estimated. It was found that the strength of joints of dissimilar hollow shafts is smaller than that of similar hollow shafts. The joint strength of solid shafts for which the outer diameter is the same as that of the hollow shafts was estimated. It was found that the strength of joints of solid shafts was larger than that for hollow shafts. In addition, it was found that the strength of joints with shafts of similar materials increases with an increase of the ratio of Young's modulus for the adherend to that for the adhesive, $E_1/E_2$.

(4) Concerning strain of the adherends, the numerical results were in fairly good agreement with the experimental results. In addition, fairly good agreement was observed between the numerical and the experimental results for joint strength. It was found experimentally that the strength of joints of dissimilar hollow shafts is smaller than that of joints of similar hollow shafts.



## References

[1] Wah, T., *Trans. ASME, J. Engineering Mater. and Technol.* **95**, 174 (1973).
[2] Adams, R. D. and Peppiatt, N. A., *J. Strain Anal.* **9**, 185 (1974).
[3] Ming-Yi Tsai and Morton, J., *Trans. ASME, Ser. E* **61**, 712 (1994).
[4] Sawa, T., Nakano, Y. and Temma, K., *J. Adhesion* **24**, 1 (1987).
[5] Temma, K., Sawa, T. and Iwata, A., *Intl. J. Adhesion and Adhesives* **10**, 285 (1990).
[6] Sawa, T., Temma, K. and Ishikawa, H., *J. Adhesion* **31**, 33 (1990).
[7] Sawa, T., Temma, K. and Tsunoda, Y., *Intl. J. Adhesion and Adhesives* **9**, 161 (1989).
[8] Temma, K., Sawa, T., Nishigaya, T. and Uchida, H., *JSME International Journal, Ser. A* **37**, 246 (1994).
[9] Nakano, Y., Temma, K. and Sawa, T., *J. Adhesion* **34**, 137 (1991).
[10] Sawa, T., Ishikawa, H. and Temma, K., *Trans. JSME, Ser. A* (in Japanese) **53**, 1685 (1987).
[11] Temma, K., Sawa, T., Ishikawa, H. and Nishigaya, T., *J. Adhesion Soc. Japan* (in Japanese) **29**, 302 (1993).